

Telemetry study of a GP2 track

Vehicle dynamics

Simone Vollaro



Corso di Laurea Magistrale in Ingegneria Robotica e dell'Automazione
Dipartimento di Ingegneria dell'Informazione
Università di Pisa

Contents

1	Preliminary operations	3
1.1	Barcelona circuit	3
1.2	Data import	3
2	Data analysis	5
2.1	Imported data	5
2.2	Raw data modification	5
2.3	Data filtering	9
3	Study of relevant quantities	11
3.1	Yaw rate	11
3.2	Slip angle	11
3.3	Lateral velocity	13
3.4	Acceleration	13
4	Circuit study	18
4.1	Centre of mass trajectory	18
4.2	Centrodes and inflection circle	18
4.3	g-g plot	22
4.4	Polar study	25
5	Data comparison	27
5.1	Comparison with real lap data	27

Chapter 1

Preliminary operations

1.1 Barcelona circuit

In this report we first study telemetry data from a simulation of the well-known Circuit de Barcelona-Catalunya, then we later compare it with telemetry data from the real circuit.

In Fig. 1.1 [Wik] we show a satellite picture of the Barcelona track taken in 2018, in which we can clearly see the outline of the newer version of the circuit.

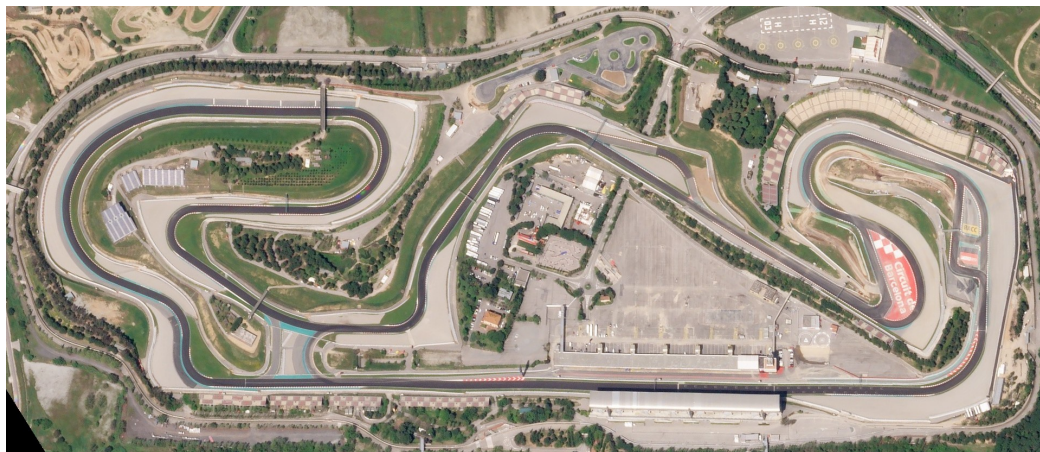


Figure 1.1: Circuit de Barcelona-Catalunya

1.2 Data import

Three files containing different telemetry data were available:

- Gp2_Barcellona_L1_SIMULATORE.xls;
- Gp2_Barcellona_L1.xls;
- Gp2_monza_L1.xls.

For the study conducted in the first part of this report, the second file has been used. As the name hints, it contains data from a simulation of the actual circuit. Although some differences could be present among different files data, the same procedure can be performed onto the other files.

Chapter 2

Data analysis

2.1 Imported data

Data gathered from the xls file show us different measurements, along with the instant in which the measure was collected.

In the Wolfram Mathematica Notebook attached to this report, these data are labeled as "raw", to underline that they are straight up from the sensors and have not been manipulated: they need to be converted into SI units, and require some tweaking in order to obtain some easily-readable plots. These changes will be presented in the next section with the proper explanations.

2.2 Raw data modification

As stated above, some changes have been made to the raw data imported. A part from the conversion to SI units, these included checking the mathematical sign of every signal to ensure proper conformity to physical conventions, and some computations needed to derive useful quantities such as lateral velocity and normal and tangential accelerations.

Corrected data are shown in Fig. 2.1 and Fig. 2.2.

As an example, in Fig. 2.3 we show the result of the former verification on the lateral acceleration a_y . Using Eq.(3.28)[[Gui18](#)] as a steady-state condition approximation, we noticed that imported data have an inverse sign.

Fig. 2.4 shows that the lateral velocity has been computed as for Eq.(7.33)[[Gui18](#)].

Further computations can be inspected in the aforementioned Wolfram Mathematica Notebook.

Figure 2.1: Telemetry data

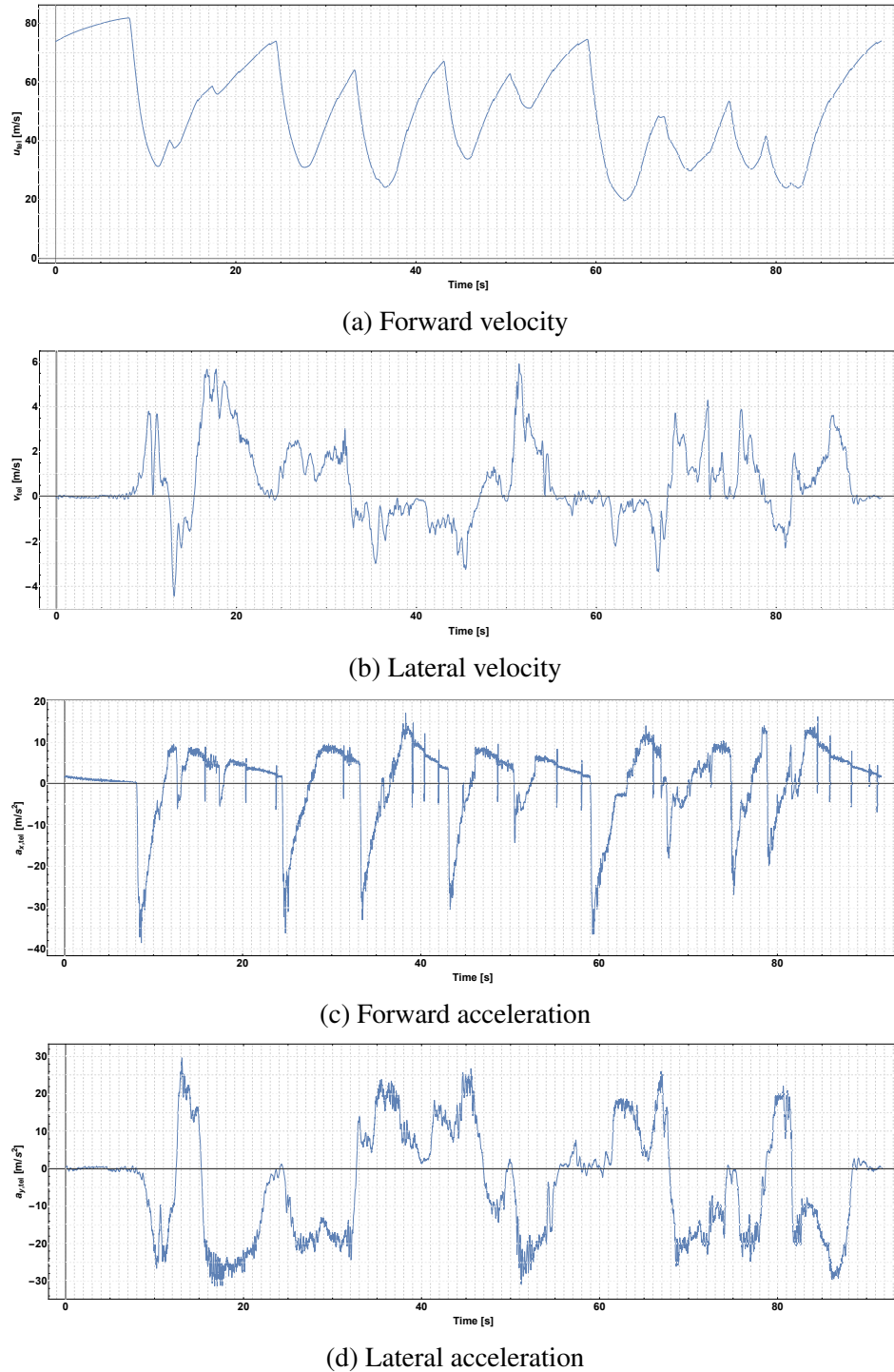
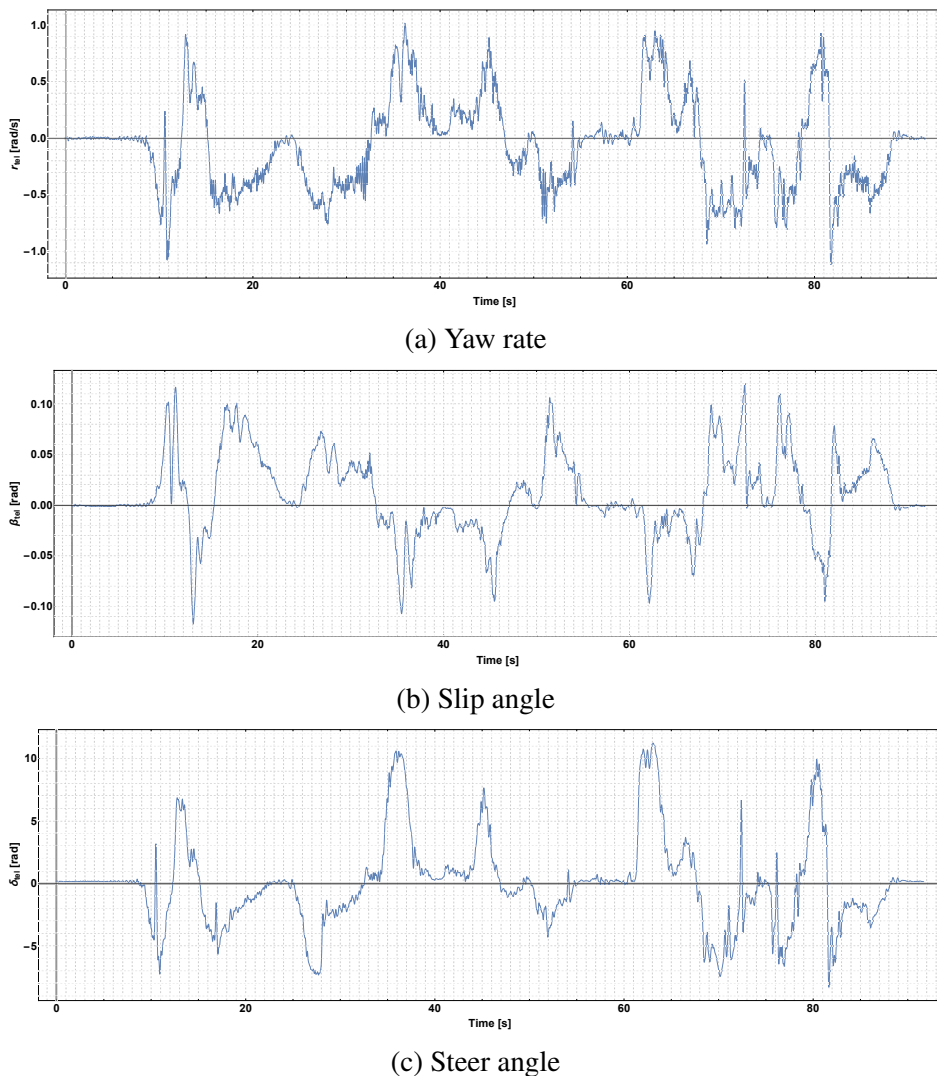
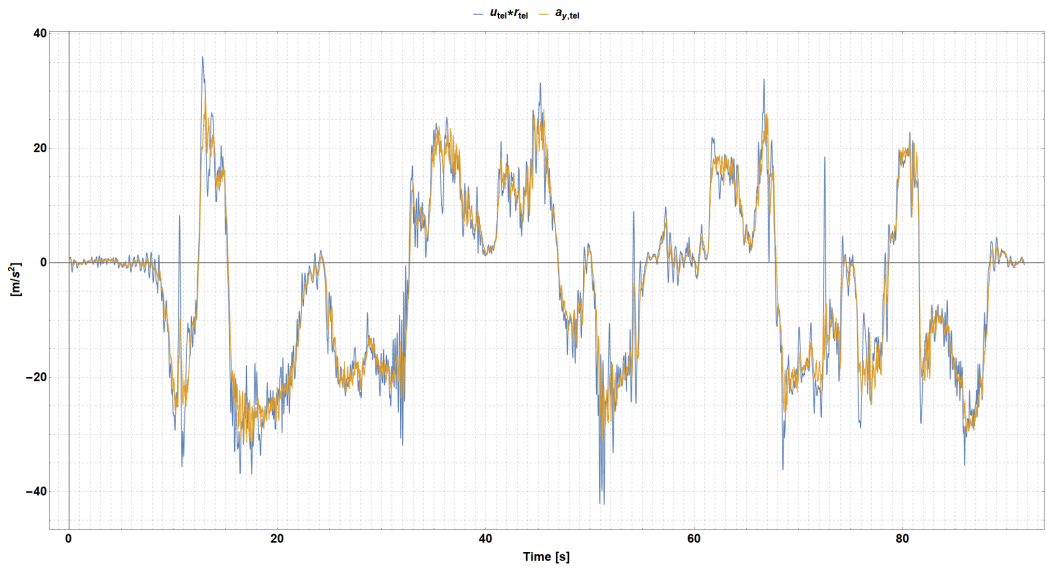
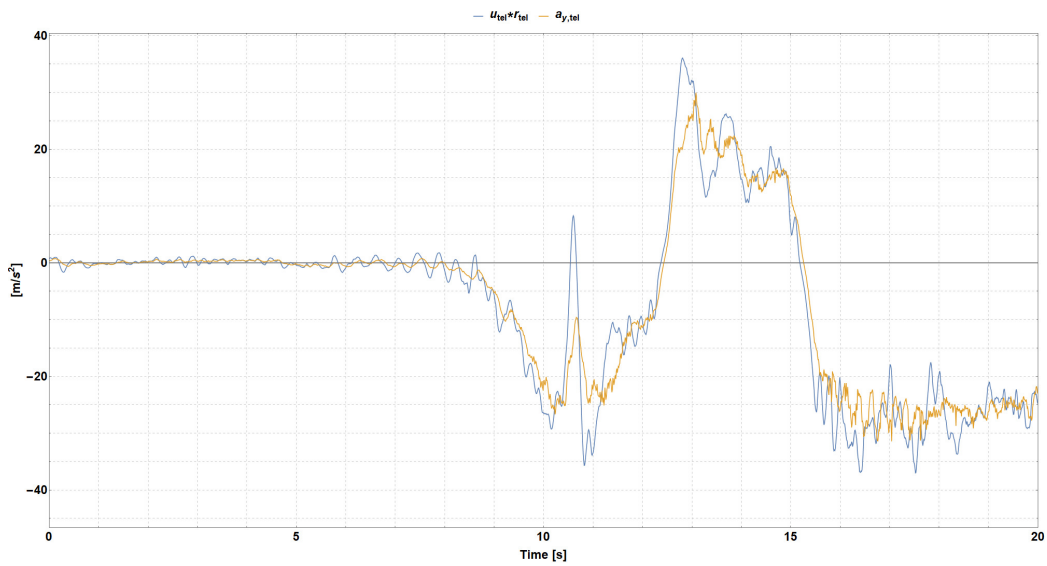


Figure 2.2: Telemetry data





(a) Whole comparison



(b) Close-up of the first 20s

Figure 2.3: Study of the lateral acceleration

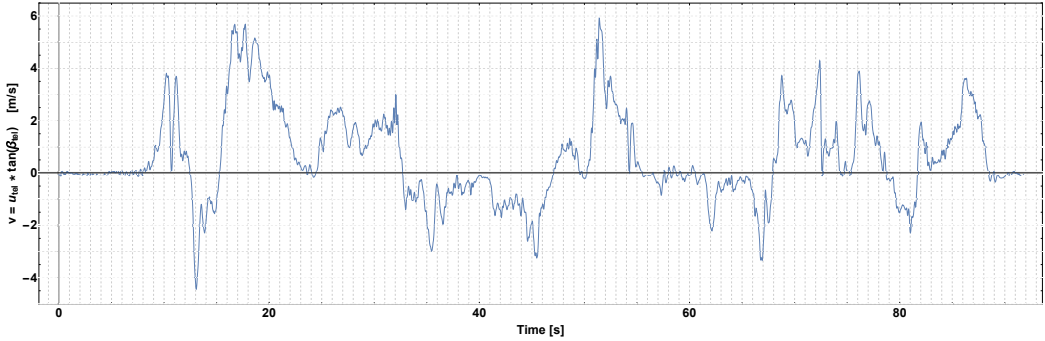
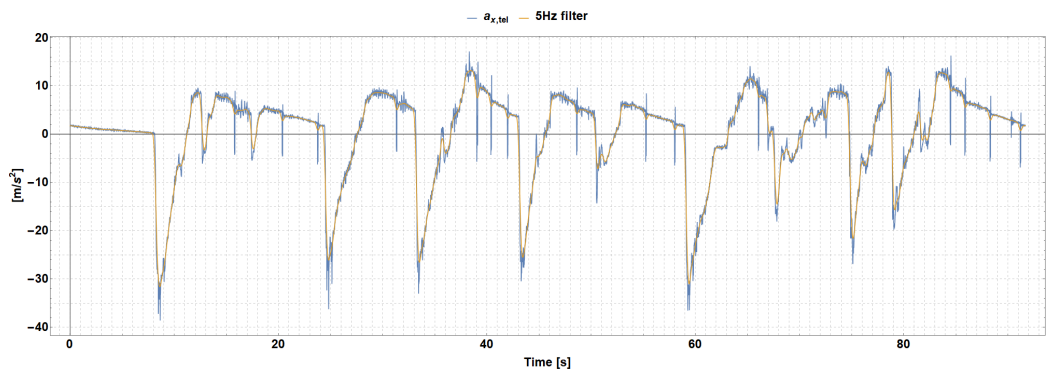


Figure 2.4: Lateral velocity, derived from other data

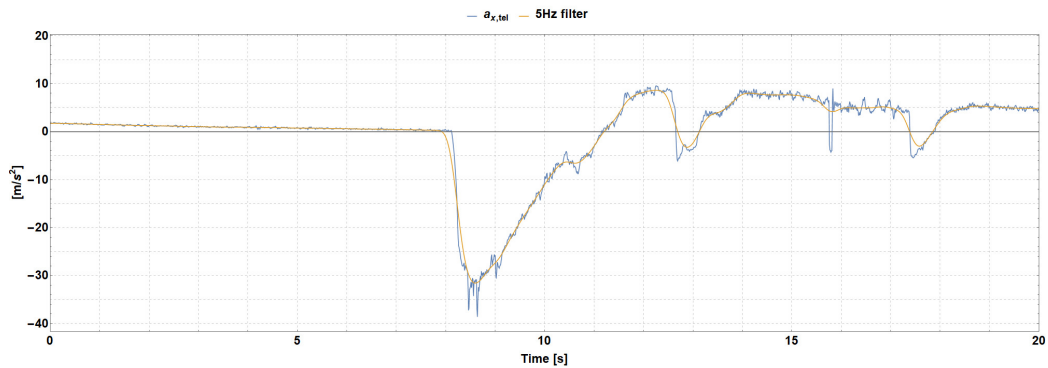
2.3 Data filtering

To remove sensor noises and disturbances, some data used in later computations have been filtered using the function *LowpassFilter*[*data*, ω_c , *n*]. For the kind of signals in exam in this work, the bandwidth of the filter has been set to 5Hz , following spectral analysis visible in the notebook but restraining ourselves to the use of a bandwidth that was not too low.

In Fig. 2.5 we show, for instance, the outcome of the designed filtering action on the forward acceleration telemetry data.



(a) Whole comparison



(b) Close-up of the first 20s

Figure 2.5: Unfiltered and filtered forward acceleration data

Chapter 3

Study of relevant quantities

3.1 Yaw rate

Once the raw data about the yaw rate has been properly corrected and filtered, it can be used to derive mathematical functions for the car yaw angle and yaw acceleration along the track (through derivative and integral operations).

Closer inspection can be carried out in the Notebook, but Fig. 3.1 shows a comparison of all three functions.

3.2 Slip angle

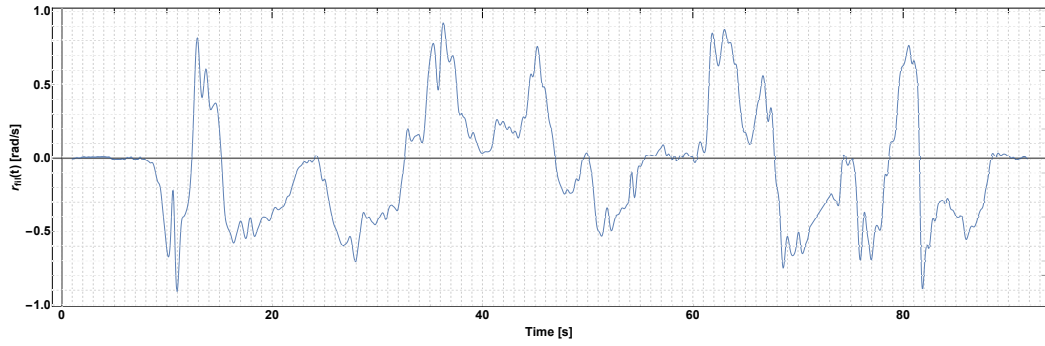
Even though it was already available among the other data, we tried to obtain the slip angle β from other quantities. Having $|\beta| \ll 1$, we chose to use the approximation given by Eq.(3.38)[Gui18]:

$$\rho_G \simeq \frac{r + \dot{\beta}}{u} \rightarrow \dot{\beta} \simeq \rho_G \cdot u - r$$

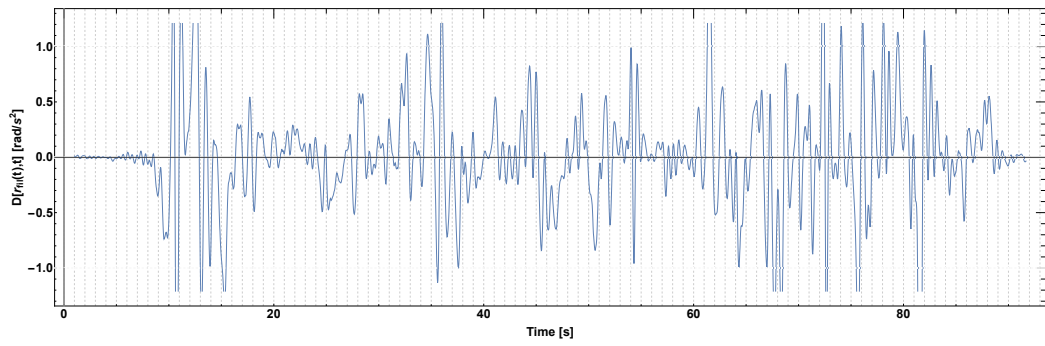
To obtain the slip angle β we then needed to integrate this formula in the time window used for gathering data.

As we can see in Fig. 3.2a, the direct integration of the above formula didn't result in acceptable quality estimations; for this reason, an ad-hoc filtration method has been carried out.

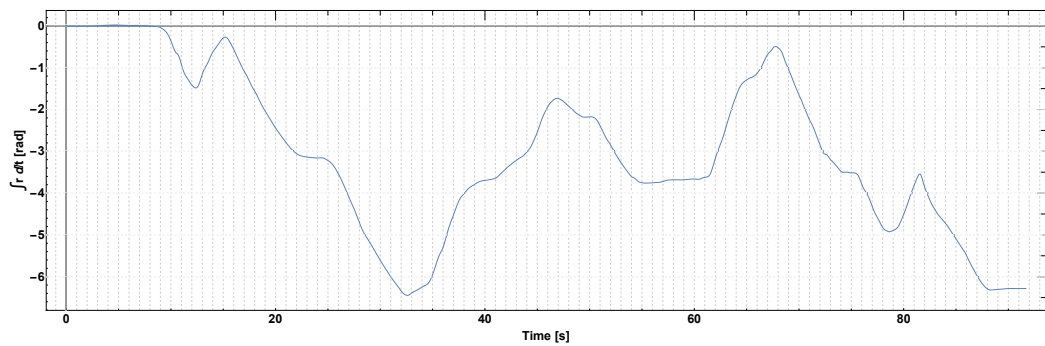
As a first step, we applied a detrendization and a *HighpassFilter*[*data*, Ω_c , *n*] to the $\dot{\beta}$ obtained through the above formula. This was meant to cancel the possible bias of the sensor used to gather data, and to filter out low-bandwidth noises, which an integration could amplify. Results from this step can be inspected in Fig. 3.2b.



(a) Yaw rate



(b) Yaw acceleration



(c) Yaw angle

Figure 3.1: Functions derived from the yaw rate study

After that, we applied a second filtration procedure. This time, a $\text{LowpassFilter}[\text{data}, \Omega_c, n]$ has been used to delete any influence of high-bandwidth disturbances, possibly deriving from the original data. Results are shown in Fig. 3.2c.

Finally, we noticed that some time ranges were showing better results in the first-step function, while other ranges were better after the low-pass filtration. This is most probably due to the fact that used cutoff frequencies (especially for the high-pass filter) were really close to the hypothesized sensor bandwidth. To obtain the best achievable estimation possible with the employed method, we then proceeded to select sub-intervals of the resulting filtered quantities, corresponding to the time intervals in which every function showed a better action on the signal. After that, we simply joined the sub-functions to obtain the final estimation. The time thresholds have been estimated to be at about 35s and 85s.

A comparison of the telemetry data and the final estimated function of β can be inspected in Fig. 3.3.

3.3 Lateral velocity

We tried to compare the function describing the lateral velocity, previously derived from gathered data, with the same quantity derived from Eq.(3.27)[Gui18]

$$a_y = \dot{v} + u \cdot r \rightarrow \dot{v} = a_y - u \cdot r$$

and integrated.

Since once again the direct integration was not satisfactory, we proceeded with another method, as done for β . This time we applied both a $\text{HighpassFilter}[\text{data}, \Omega_c, n]$ and a $\text{LowpassFilter}[\text{data}, \Omega_c, n]$ during the integration computations. Estimated thresholds were at about 20s and at 86s.

We show the result of the process in Fig. 3.4.

3.4 Acceleration

Finally, before focusing on the car movements on the circuit, it was necessary to have a closer look to the acceleration data.

We implemented interpolating functions to confirm Eq.(3.26)[Gui18] and Eq.(3.27)[Gui18], comparing acceleration data with computations made from other quantities. Fig. 3.5 shows that gathered data are consistent with those equations.

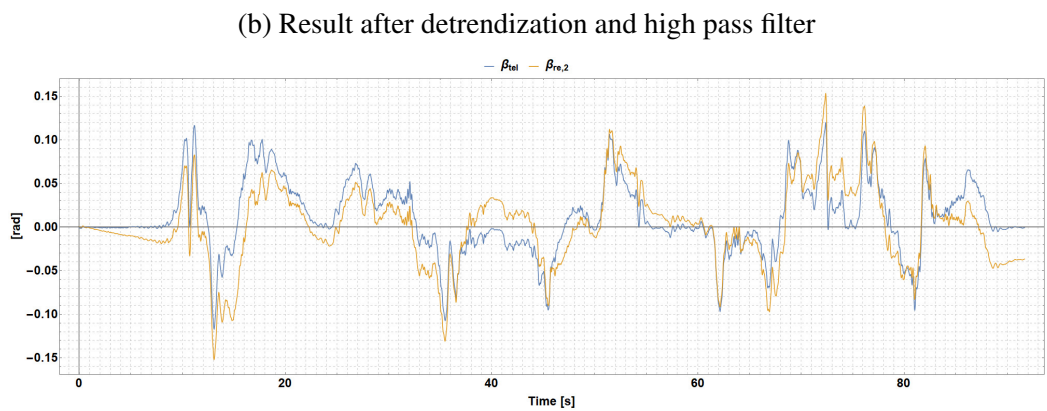
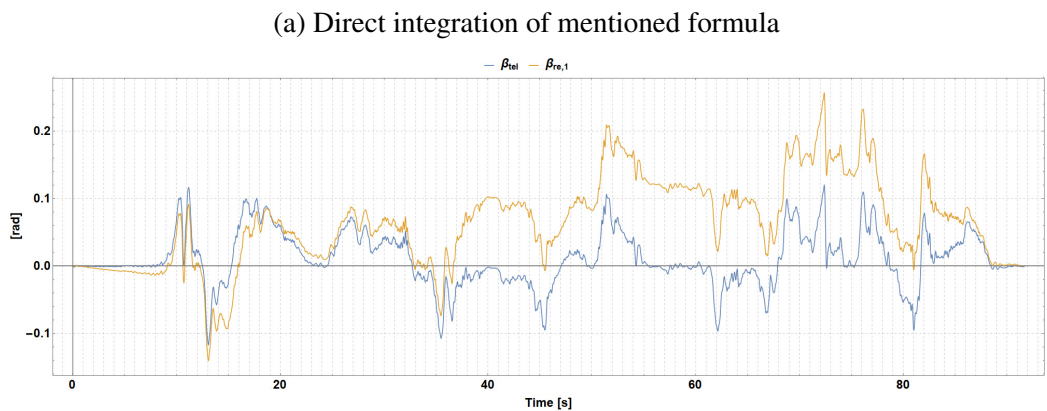
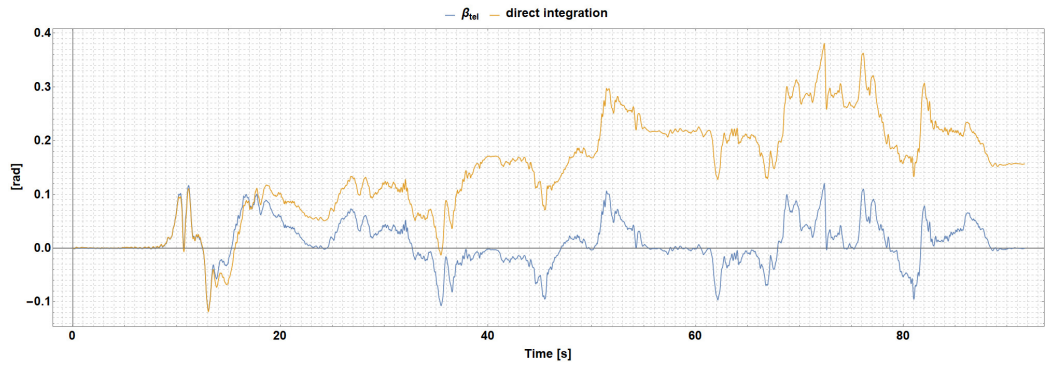


Figure 3.2: Study to obtain the slip angle β

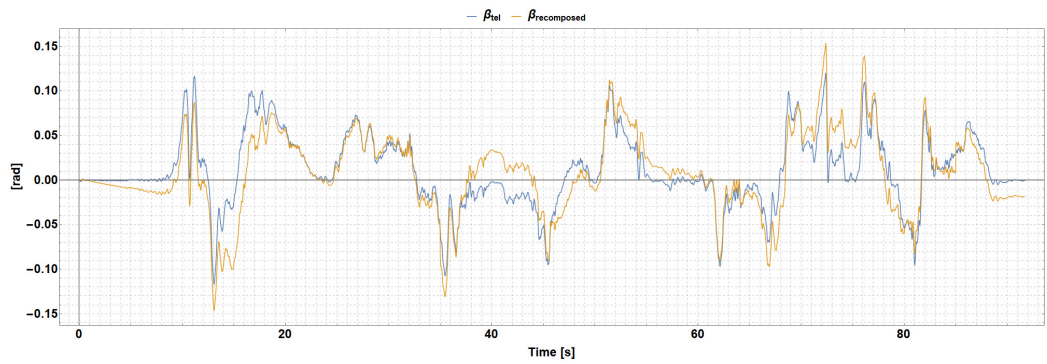


Figure 3.3: Comparison of β data and estimate

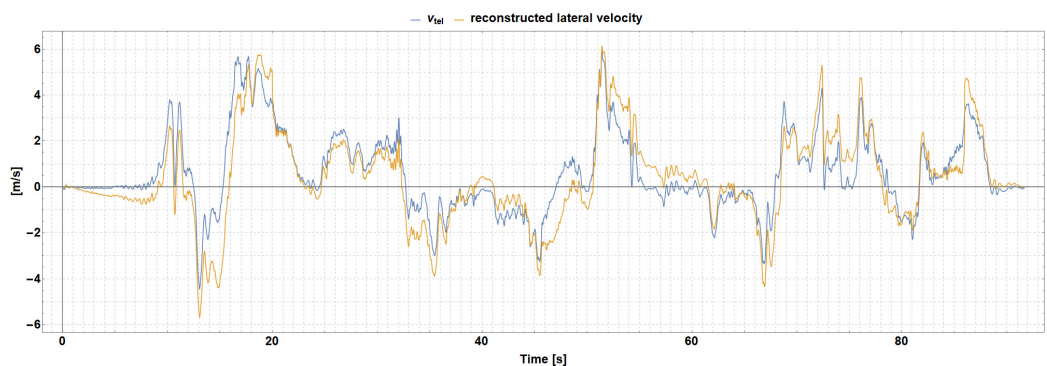
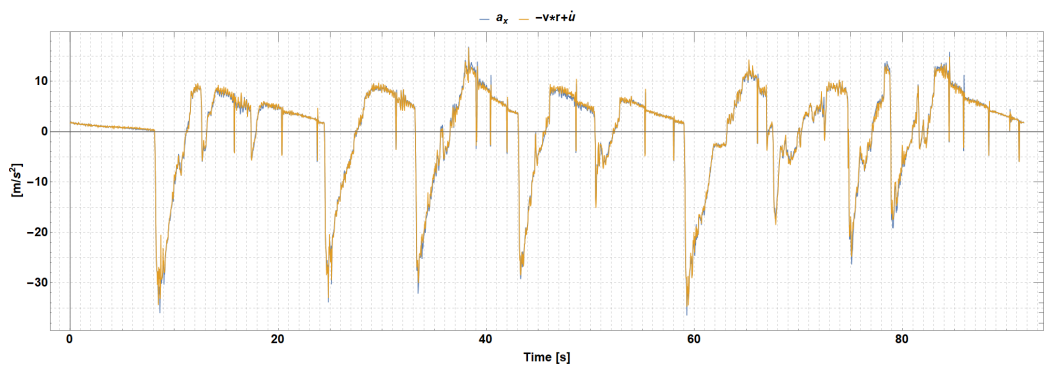
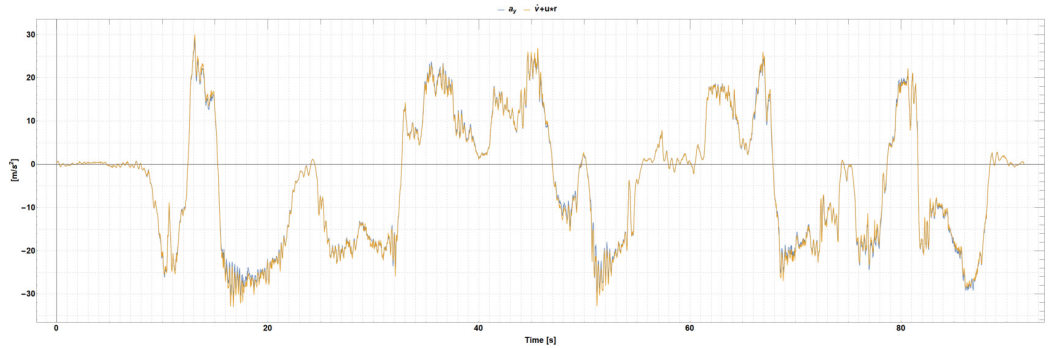


Figure 3.4: Lateral velocity functions comparison



(a) Forward acceleration



(b) Lateral acceleration

Figure 3.5: Acceleration data

After that, we used the same aforementioned equations (with some computations) to once again derive the slip angle β , from

$$u \cdot \dot{\beta} + \beta \cdot (a_x + v \cdot r) = a_y - u \cdot r$$

Even though we also applied filtering functions to the result, Fig. 3.6 clearly shows that the attempt to derive the slip angle in an indirect way is not advisable, if a fine-tuning of the filtering functions is not accomplished.

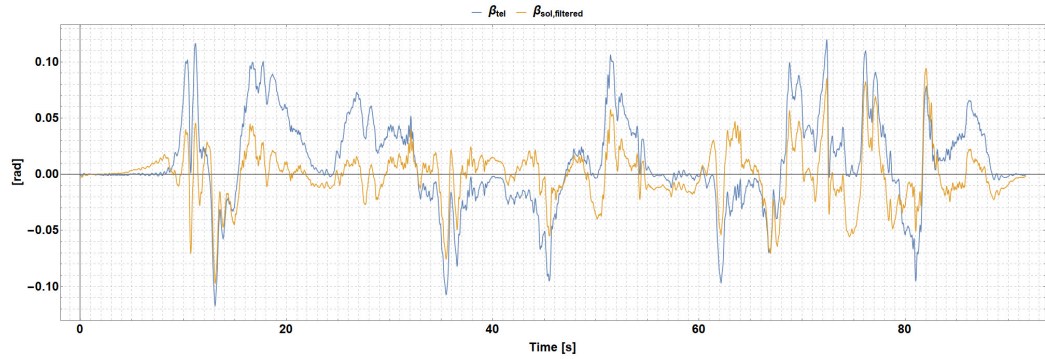


Figure 3.6: Attempt to derive the slip angle from acceleration data

Chapter 4

Circuit study

4.1 Centre of mass trajectory

After obtaining the lateral velocity v in a previous chapter, we can reconstruct the coordinates of the vehicle's centre of mass in the fixed frame with Eq.s(3.9)[Gui18].

To get a more precise result, it is a good idea to average a clockwise and a counterclockwise lap of the track (inverting the data lists used).

Fig. 4.1 shows the reconstructed track of the vehicle's centre of mass. The fact that the obtained circuit is not a closed curve is caused by the influence of errors and disturbances, and was therefore expected.

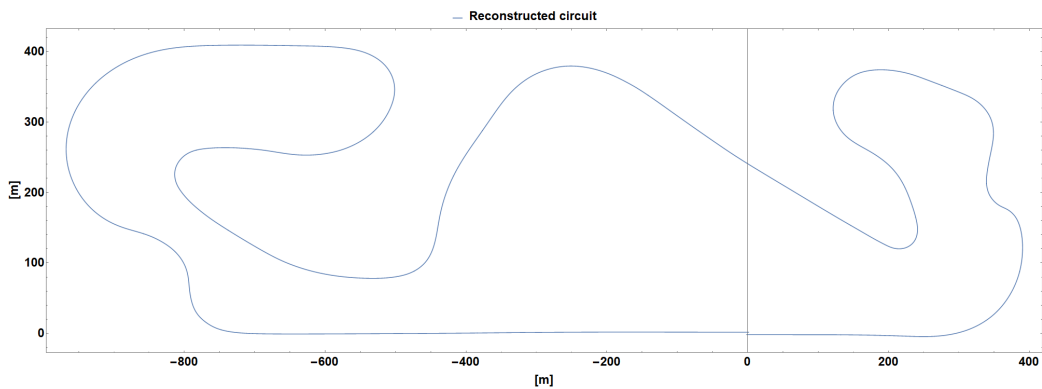


Figure 4.1: Reconstructed circuit

4.2 Centrodes and inflection circle

We can compute the fixed and moving centrodes of each curve approached by the vehicle with Eq.s(5.12)[Gui18] and Eq.s(5.13)[Gui18]. In the same way,

Eq.s(5.14-5.17)[[Gui18](#)] are used to compute the centre and the radius of the inflection circle at each turn, which was then plotted with standard circumference graphic functions.

Figures [4.2](#) through [4.4](#) shows all elements of each curve computed at a random instant of time. Complete animations can be inspected in the Notebook.

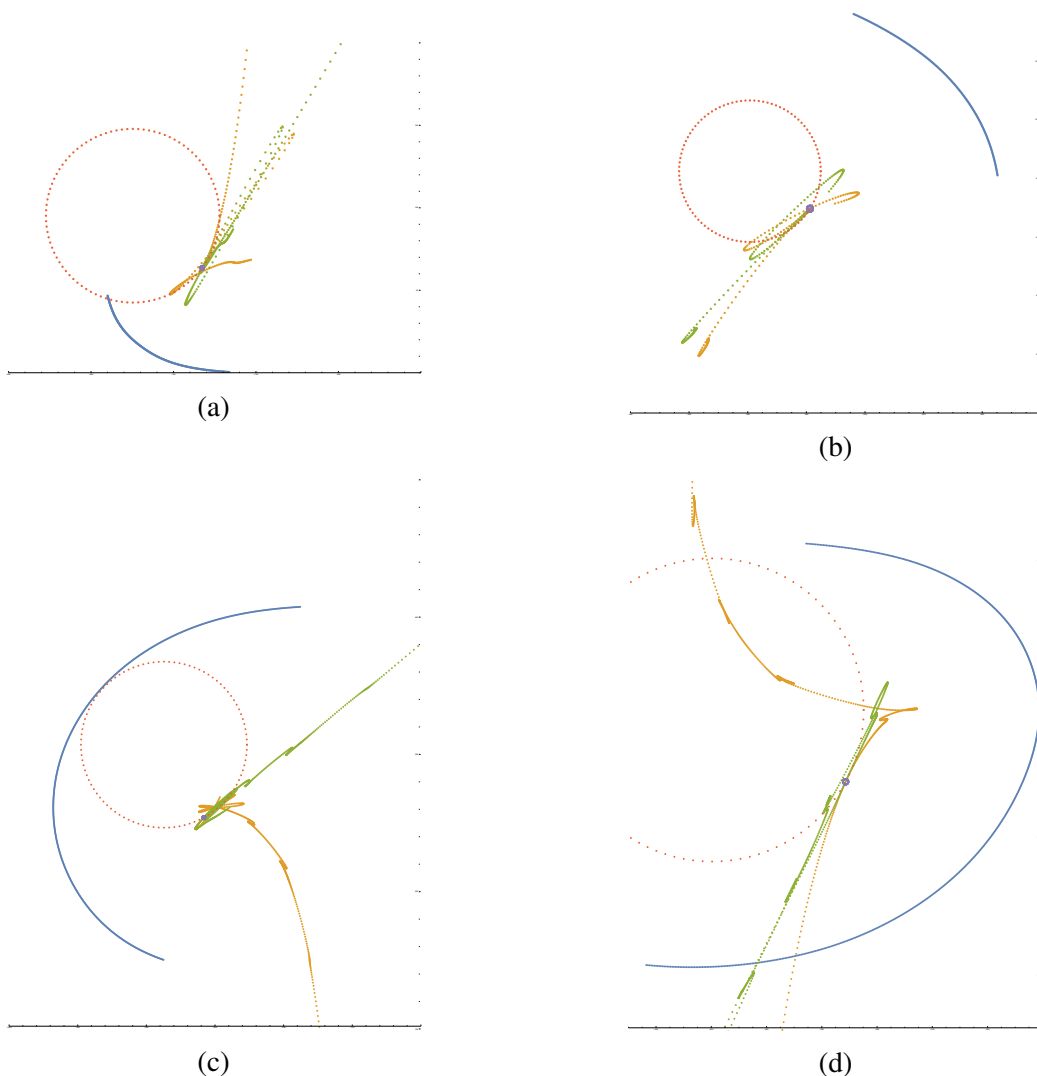


Figure 4.2: Turns 1 to 4

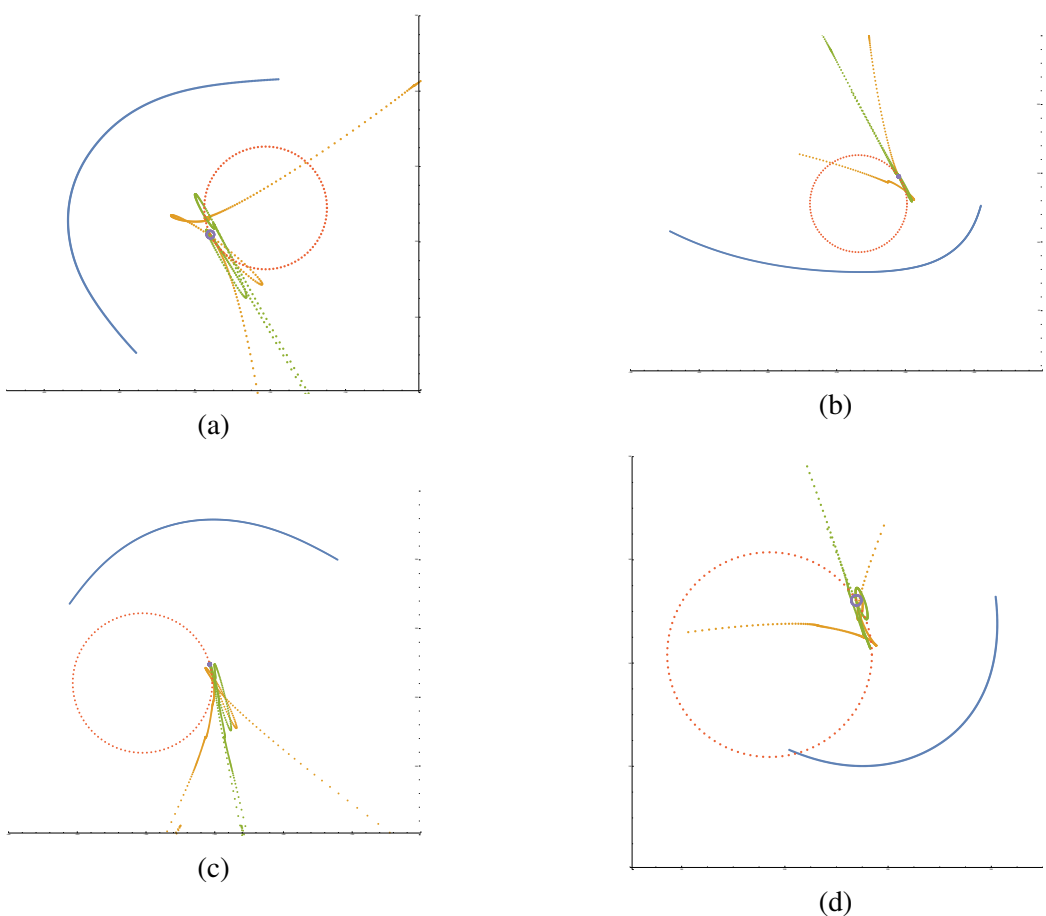


Figure 4.3: Turns 5 to 8

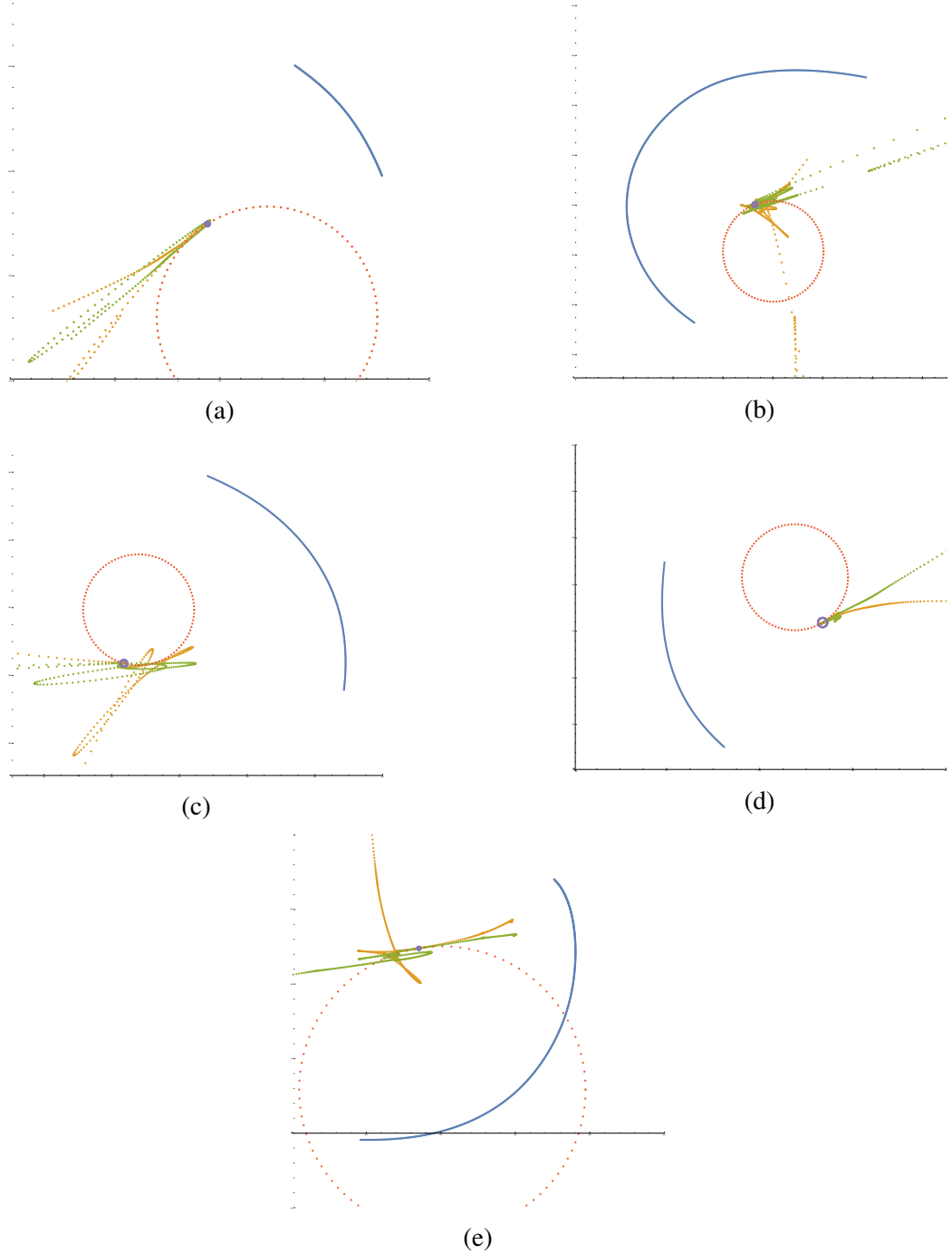


Figure 4.4: Turns 9 to 13

4.3 g-g plot

Under ideal conditions, acceleration data gathered from a racing car should be distributed onto what is called "friction circle". This circle should help visualize the maximum achievable tires grip of the vehicle during the studied track. Fig. 4.5 shows an example of said friction circle.

However, in practice this area is less clear than a proper circle. Since real cars have much more ability to stop than to go, it normally looks more like a laying down capital "D" shape.

Fig. 4.6 shows the g-g diagram of the lap studied, along with a convex hull encasing the data, in place of the friction circle.

This polygonal hull is obtained through the function *ConvexHull[data]*: it is the smallest convex set that includes all data points. In practice, it has the same function of the ideal friction circle: since it is computed through a mathematical data analysis, it symbolizes the maximum longitudinal and lateral force (or acceleration, in an equivalent way) that the observed car could have achieved during the lap.

A complete animation can be inspected in the Notebook.

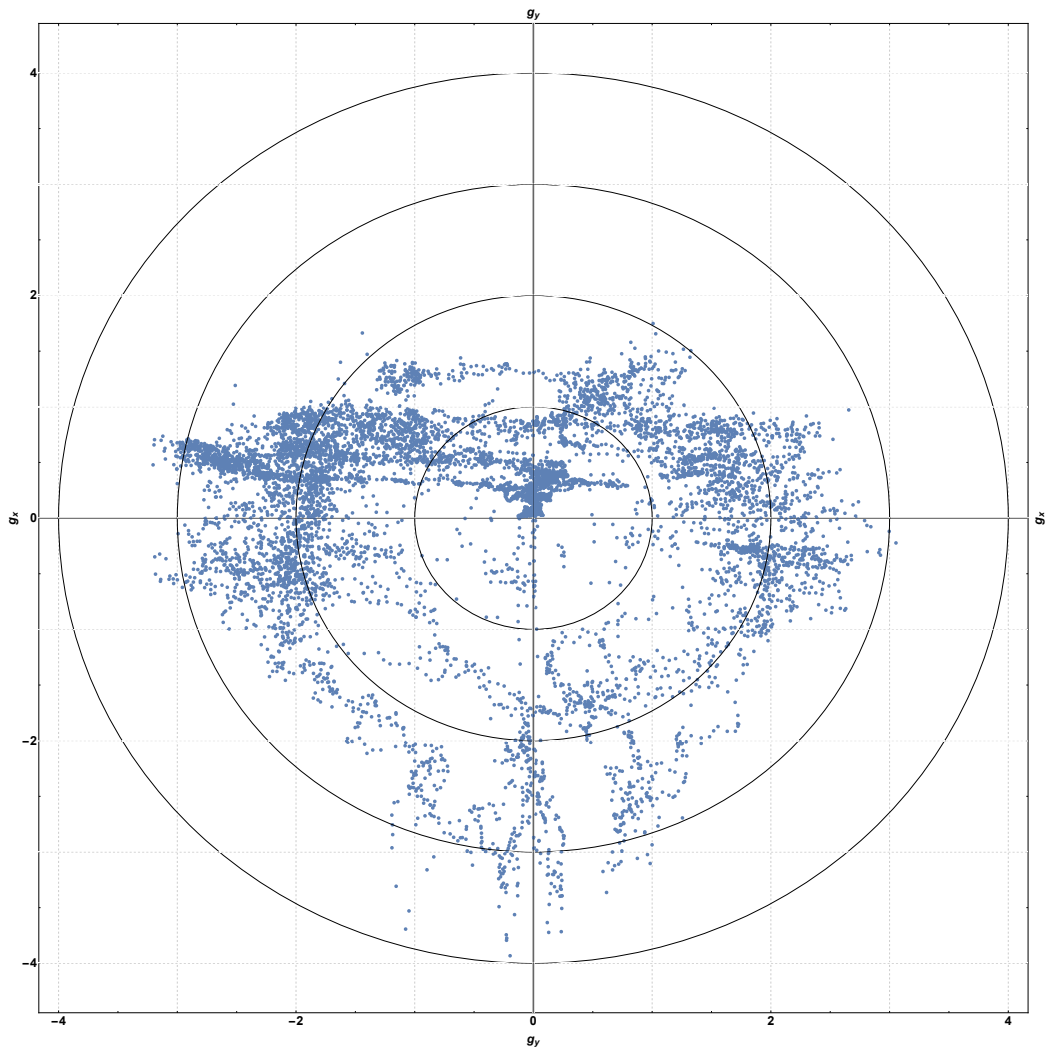


Figure 4.5: g-g plot with classic friction circle

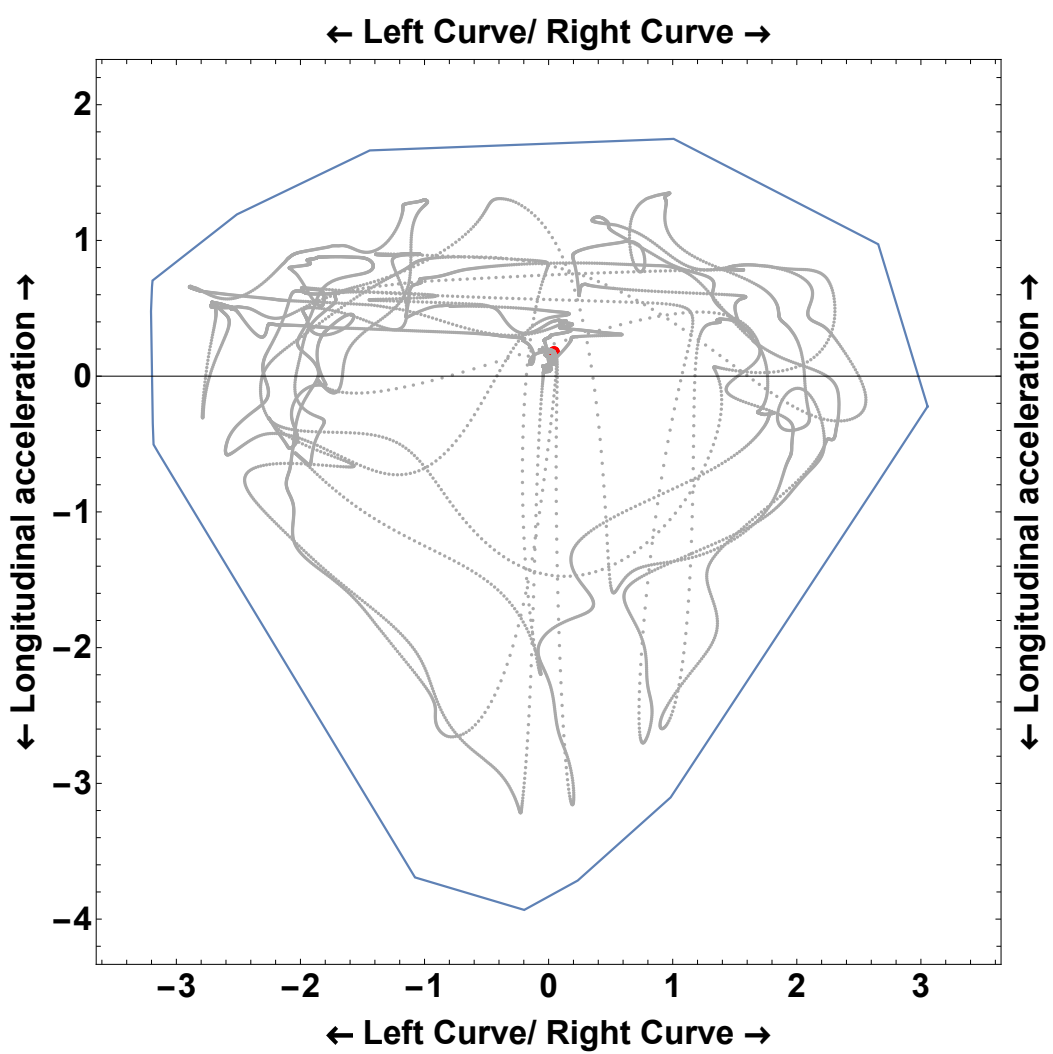


Figure 4.6: g-g diagram with real data

4.4 Polar study

In this section we provide a brief examination of the vehicle approach to a turn, taking curve 5 as example. Fig. 4.7 will be referred to in the following analysis.

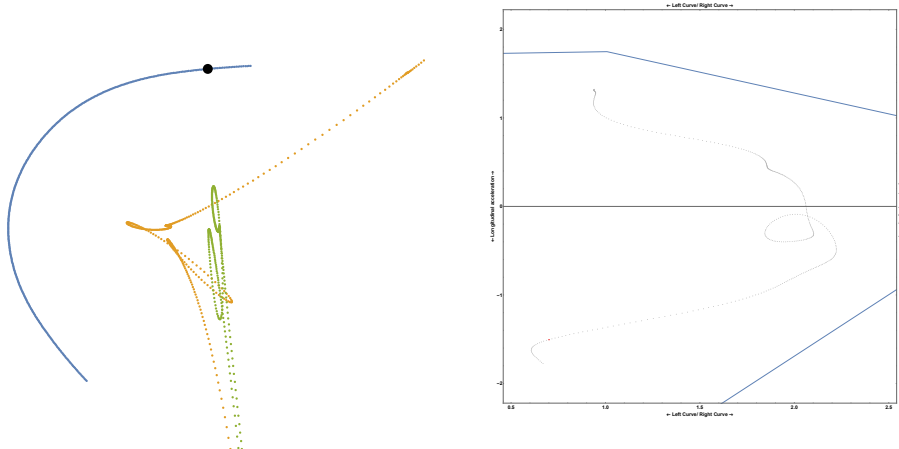


Figure 4.7: Centrodes and g-g plot points relative to the considered turn

The first thing to notice is that the fixed and moving centrodes are not quite smooth: they even present some ripples [Fig. 4.8a]. This can be explained by analysing the vehicle behaviour in the curve, in order to pinpoint the possible cause in the way the driver is piloting the car.

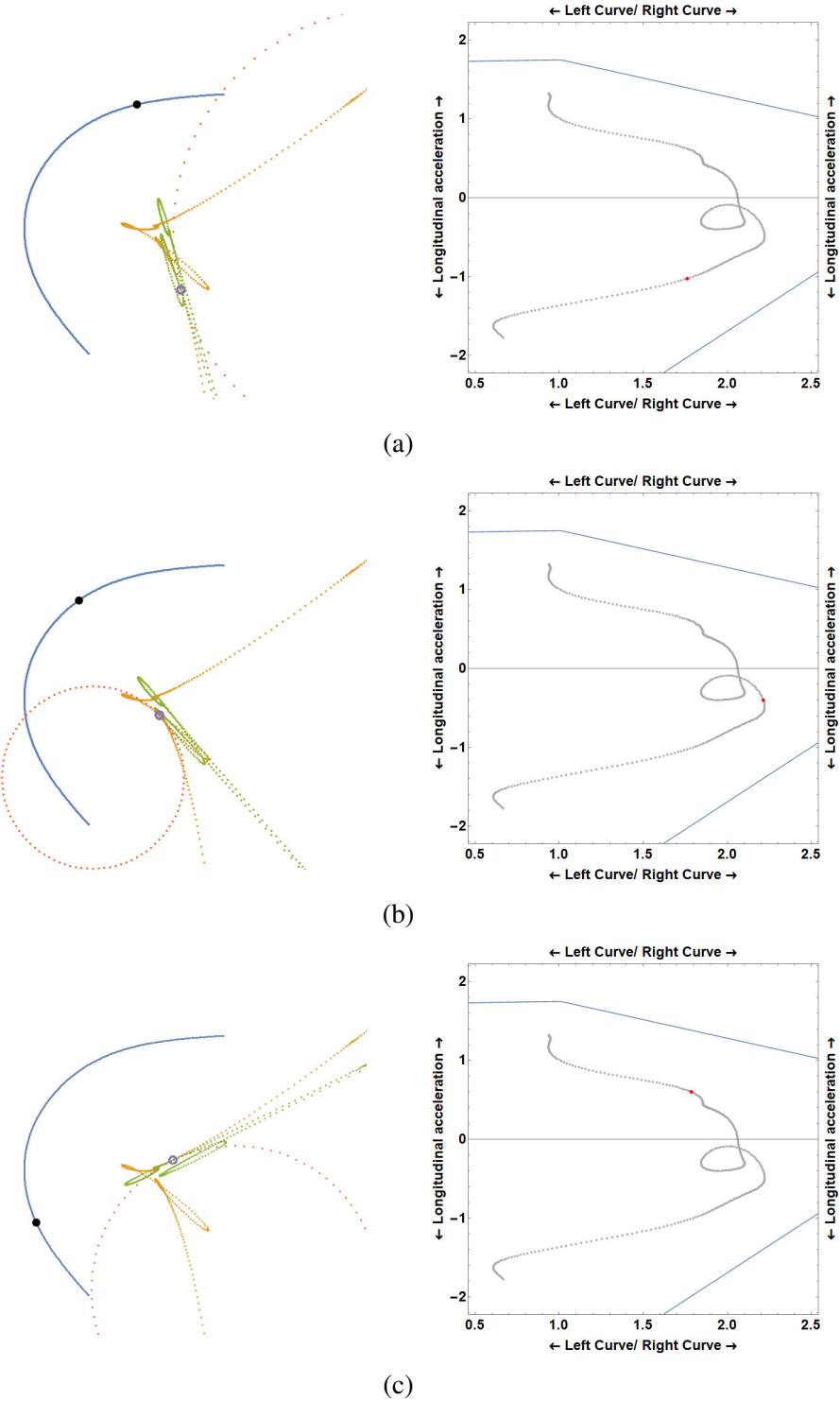
We can notice that up until the first third of the curve the driver is still turning right even though this is a left-hand turn. Probably due to a misalignment of the car from the path the pilot is willing to follow, this is not a surprising behaviour: in a normal situation, curves are almost never approached optimally (in the sense of "following the right path"), so most of the time drivers have to adjust the heading direction while entering the curve.

At this point, we can see in Fig. 4.8b that the first ripple in the polar plots is caused by the change of direction after the aforementioned realignment.

That is also the same source of the successive ripples: judging by the points outline in the g-g plot, the driver is probably realigning the car, considering its orientation not good enough for the exiting phase.

Finally, as shown in [Fig. 4.8c], the car accelerates and tackle the last part of the curve. This causes the last staggering effect of the centrodes, indicating a hesitant acceleration.

Figure 4.8: Relevant parts of the turn approach



Chapter 5

Data comparison

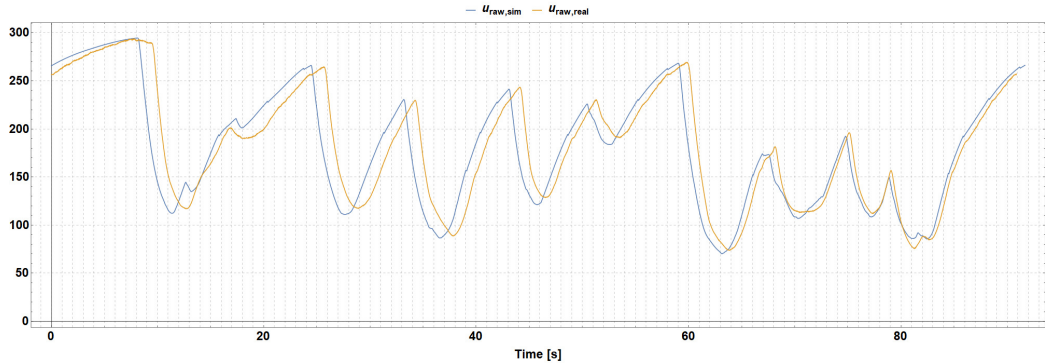
5.1 Comparison with real lap data

In this final section we compare telemetry data previously studied with other data gathered from a real vehicle completing a lap in the actual Barcelona circuit. Since the whole procedure followed in the previous chapters would be the same, with the result of only changing some numerical parameter (i.e. filter bandwidths), we here restrict ourselves to only a comparison of the raw data obtained from the sensors. Comparison plots are shown below.

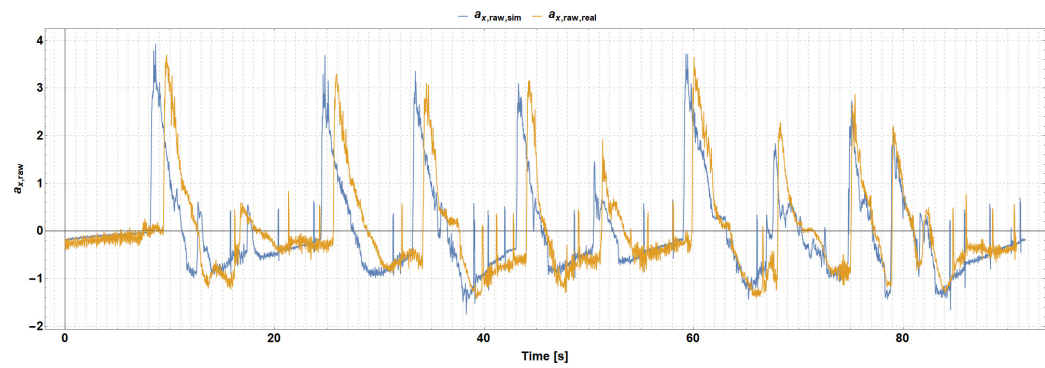
The first thing we can notice is that all data from the real circuit is apparently delayed of about 1s with respect to simulation data. This is most probably the consequence of the behaviour of a real vehicle in place of a simulated one: even if the driver presses the acceleration pedal to its end at the start of the lap, friction and other dissipation-like effects (i.e. mechanical resistances) drag the car down and prevent it from moving free as in the simulation. This happens even if the simulation is already including a friction model: real-life behaviour is unavoidably different.

On a side note, we can also consider the fact that it is unknown if the person driving the real vehicle is the same one of the simulation, nor if they are expert pilots or only everyday drivers. Both these annotations would add some information to the context, allowing us to analyze deeper the gathered data and the vehicle performances on the track.

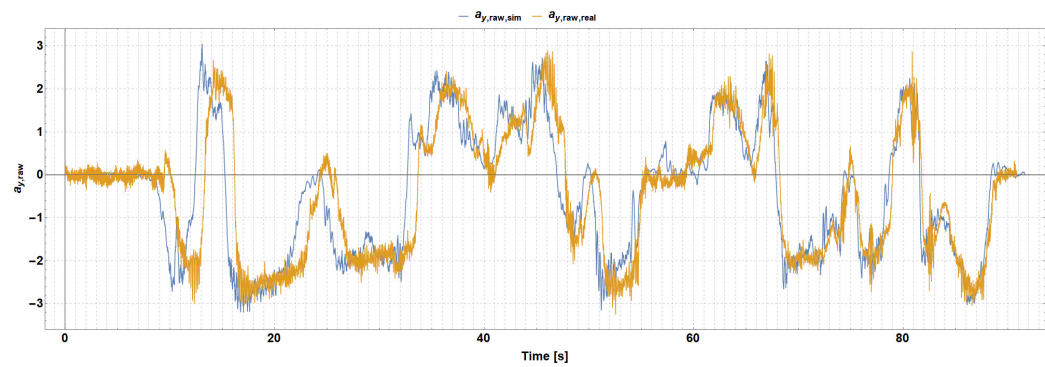
Having a closer look, we can clearly see in Fig.s [5.1a-5.1b-5.1c](#) that data for the longitudinal velocity and lateral and longitudinal accelerations are similar between the two telemetries. For all of them, the data ranges are equivalent and the general outline are very close one another, so it is fair to assume they are also



(a) Longitudinal velocity comparison



(b) Longitudinal acceleration comparison



(c) Lateral acceleration comparison

Figure 5.1

gathered with the same unit of measure. The only relevant difference is in the influence of noises and disturbances: real-life measurements are obviously more affected by them, clarifying that the model used in the simulation is probably not too accurate.

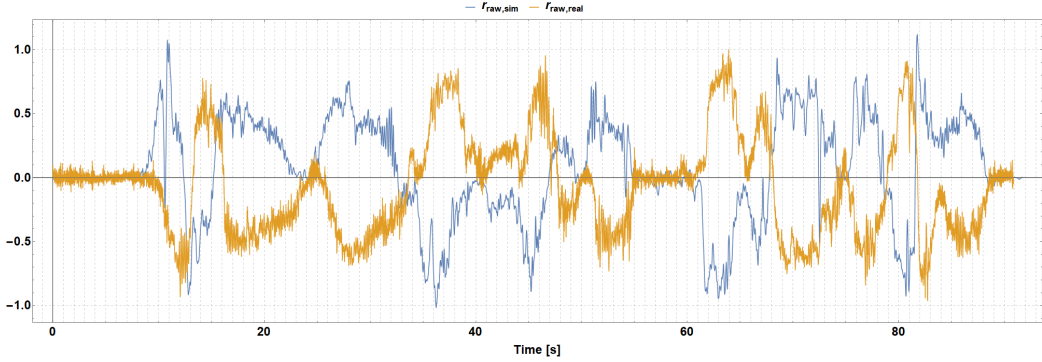


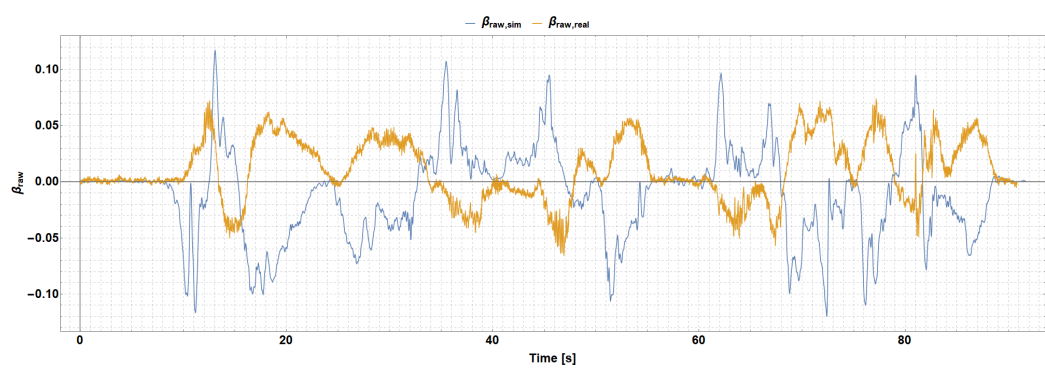
Figure 5.2: Yaw rate comparison

The plot in Fig. 5.2 has been generated adapting real telemetry data to the simulation one. Whilst it can be seen that they are in the same range despite the greater noise, we must consider that real data have been gathered with an inverse sign and a different unit of measure (degree instead of radians) with respect to the simulation. That's the reason an adaptation was needed in the first place to compare the two sets.

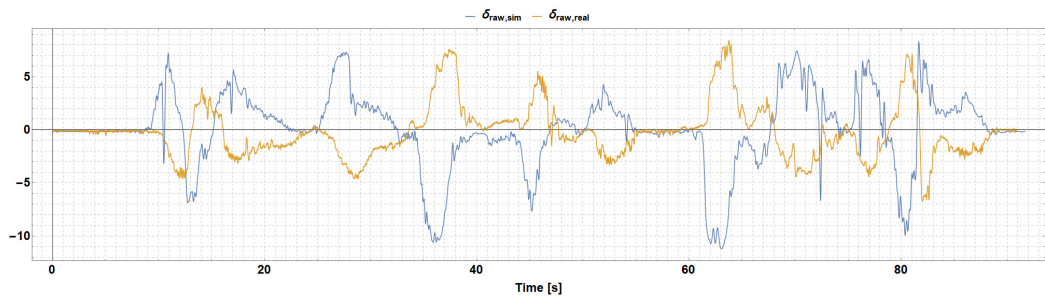
A likely explanation of the aforementioned differences in yaw rate data can be the use of different sensors between the real vehicle and the simulation platform (supposing this is not entirely software).

Fig.s 5.3a-5.3b shows that real data for the slip angle and the steer angle, as the yaw rate before, have been gathered with an inverse sign. The slip angle plot have been adapted as in the case of the yaw rate, since once again the unit of measurement was different.

The lower intensity of the real signal, respect to the simulated data, suggests once more a greater influence of noises and uncertainties onto the used sensor.



(a) Slip angle comparison



(b) Steer angle comparison

Figure 5.3

Bibliography

- [Gui18] Massimo Guiggiani. *The Science of Vehicle Dynamics. Handling, Braking, and Ride of Road and Race Cars.* 2nd Edition. 2018.
- [Wik] Wikipedia.org. *Circuit de Barcelona-Catalunya.* URL: https://en.wikipedia.org/wiki/Circuit_de_Barcelona-Catalunya.